LAWRENCE
LIVERMORE
NATIONAL
LABORATORY

UCRL-CONF-222392

CHARACTERIZATION OF DAMAGED MATERIALS

P. C. Hsu, M. Dehaven, M. McClelland, S. Chidester, J. L. Maienschein

June 23, 2006

13th International Detonation Symposium
Norfolk, VA, United States
July 23, 2006 through July 28, 2006

CHARACTERIZATION OF DAMAGED MATERIALS

Peter C. Hsu, Martin Dehaven, Matthew McClelland,
Steve Chidester and Jon Maienschein

Lawrence Livermore National Laboratory
Livermore, CA 94550

Thermal damage experiments were conducted on LX-04, LX-10, and LX-17 at high temperatures. Both pristine and damaged samples were characterized for their material properties. A pycnometer was used to determine sample true density and porosity. Gas permeability was measured in a newly procured system (diffusion permeameter). Burn rate was measured in the LLNL strand burner. Weight losses upon thermal exposure were insignificant. Damaged pressed parts expanded, resulting in a reduction of bulk density by up to 10%. Both gas permeabilities and burn rates of the damaged samples increased by several orders of magnitude due to higher porosity and lower density. Moduli of the damaged materials decreased significantly, an indication that the materials became weaker mechanically. Damaged materials were more sensitive to shock initiation at high temperatures. No significant sensitization was observed when the damaged samples were tested at room temperature.

INTRODUCTION

Safe handling of explosives requires a sound understanding of the circumstances in which various stimuli might lead to an undesired ignition. Examples of stimuli are accidents caused by fire, earthquakes, and problems associated with operational handling, transportation, sudden climate change, and combat operations in battlefields. These can expose energetic materials to unexpected thermal and mechanical impacts that may damage the explosive charge (e.g., change composition, microstructure, introduce voids and porosity). This may affect material properties, safety and performance of explosives.

Mechanical damage comes from tensile or shear stresses associated with rigorous vibration, or high-rate impact. This may cause deformation and cracking of the energetic material, which could change its mechanical properties (strength, modulus, Poisson's ratio) and physical properties. When energetic material is subjected to unexpected heat, the thermally induced off-gassing or other thermal effects at elevated temperature may result in micro cracking, voids, defects, and thermal expansion. It may also result in a phase change (e.g., beta to delta transition in HMX). The thermal damage may have a significant effect on the chemical properties and physical properties (surface area, porosity, density, gas permeability). The resulting damaged explosives may be more sensitive to shock or impact initiation, may be more thermally sensitive, and may react more violently when reaction begins.

LX-04, LX-10, and LX-17 were developed by the Lawrence Livermore National Laboratory. LX-04 and LX-10 are HMX-based plastic-bonded explosives, which consist of 85% wt. and 95% wt. of HMX, respectively, and balance of binder (Viton A). LX-17 is a TATB-based plastic-bonded explosive which consists of 92.5% wt. of TATB and 7.5% wt. of binder (Kel-F 800). In this paper, we will describe our approach and share our recent experimental results on LX-04, LX-10, and LX-17.

MEASUREMENT OF MATERIAL PROPERTIES

Material properties affect safety and performance of explosives Working principles for measuring several relevant material properties are described below.

Gas Permeability in Energetic Materials

Gas permeability data are important in modeling the performance of explosives. According to Darcy's law, flow of fluids through porous media is proportional to the pressure gradient causing flow, as shown in equation 1 [1]:

$$V = - Ø (\partial P/\partial X) \quad (1)$$

The proportionality constant ø is a function of the fluid viscosity as expressed by equation (2):

$$V = - (K/\mu) (\partial P/\partial X) \quad (2)$$

which can be written in the more convenient form

$$F = A (K/\mu) (P_i - P_o)/L \quad (3)$$

Where:
V = fluid liner flow rate in volume per surface area per time, cm/sec
Ø = permeability, cm^4/dynes/sec
K = specific permeability, cm^2
μ = fluid viscosity, dynes.sec/cm^2
P = fluid pressure, dynes/cm^2
X = distance in the direction of fluid flow, cm
F = fluid flow rate in volume per time at average pressure, cm^3/sec
A = cross-sectional area perpendicular to the direction of fluid flow, cm^2
P_i, P_o = fluid pressures in the upstream and downstream, respectively, dynes/cm^2
L = thickness of the porous media for fluid transport, cm

The specific permeability of gas in materials is calculated by equation (4):

$$K = F_s (2\mu L P_s T)/(A T_s (P_i + P_o)(P_i - P_o)) \quad (4)$$

Where:
F_s = gas flow rate in volume per time at standard pressure and room temperature, cm^3/sec
P_s = standard pressure, 1.0133×10^6 dynes/cm^2
T = gas temperature, ^oK
T_s = room temperature, 298.15 ^oK

Surface Area Measurement by Gas Adsorption

When a clean surface is exposed to a gas, an adsorbed film forms on the surface. The amount of gas adsorbed depends on several factors like temperature, pressure, and the interaction potential. Chemical adsorption is irreversible and involves the chemical bonding of the gas or vapor to the surface of the material. On the other hand physical adsorption is reversible and exhibit characteristics that make it more suitable for surface area measurements.

The BET (Brunauer, Emmett, Teller) theory for surface area measurement is made by predicting the number of adsorbate molecules required to cover the solid with single monolayer [2]. The effective cross sectional area of the molecule is then used to calculate the surface area. In reality, there exists no pressure at which the surface is covered with exactly a completed physically adsorbed monolayer. The effectiveness of the BET theory is that it enables an experimental determination of the number of molecules required to form a monolayer despite the fact that exactly one monomolecular layer is never actually formed. The determination of the surface area from BET theory is a straightforward application of the following equation derived from the classical Langmuir isotherm.

$$1/(V(P_0/P - 1)) = 1/(V_m C) + (C-1)/(V_m C) (P/P_0) \quad (5)$$

Where
P = pressure of the vapor
P_0 = equilibrium vapor pressure at the system temperature
V = amount of adsorbed gas, cc (stp)/g solid
V_m = amount of gas that can form a monolayer, cc (stp)/g solid
C = a dimensionless constant that depends upon temperature and the properties of the vapor and the surface

A plot of $1/V[(P_0/P)-1]$ versus P/P_0 will usually yield a straight line in the range $0.05 \leq P/P_o \leq 0.35$. The slope s and the intercept i of the BET plot are given by

$$s = (C-1)/(V_m C) \quad (6)$$

$$i = 1/(V_m C) \quad (7)$$

Solving equations (6) & (7) yields

$$V_m = 1/(s+i) \quad (8)$$

$$C = (s/i) + 1 \quad (9)$$

The surface area of the material is then given by

$$S = V_m A/22400 \quad (10)$$

Where
S = specific surface area of solid, cm^2/g
A = cross-sectional area of the adsorbate gas, cm^2/mole
22400 = molar volume of adsorbate gas at stp (1 atm, 0^o C), cc/mole

Pores and Voids

Voids and pores exist in a material structure. Figure 1 illustrates three different types of pores that may be observed: blind pores, closed pores, and through pores. A channel formed by the pores may start from one surface and terminate inside the material. Such pores are called *blind pores*. Blind pores influence the amount of fluid that can be stored in the material. Blind pores contribute to the increase in surface area and the decrease in density. When the pore is completely enclosed inside the material, it is called *closed pore***.** The presence of closed pores reduces the material density, but do not contribute to flow through the material. The channels that extend from one free surface of the material to another are called *through pores.* Through pores are responsible for fluid flow through the material. Through pores also contribute to the increase in surface area and the decrease in material density.

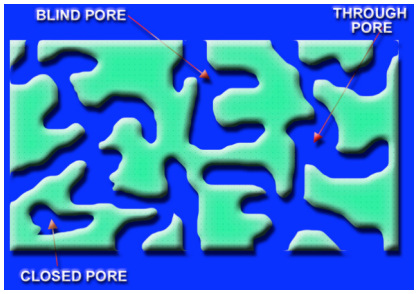

FIGURE 1. Closed pore, blind pore, and through pore in a porous material structure [3].

Measurements of Pore Size and Pore Size Distribution

Mercury intrusion is a traditional technique used for measuring porosity of a porous material based on the amount of mercury intruding into the pores of the material with increase in mercury pressure. Due to its toxicity, non-mercury liquid intrusion technique has been developed recently and instruments are available commercially. Non-mercury liquid intrusion technique utilizes non-wetting liquid and applies pressure to force the non-wetting liquid into pores of a sample. The pressure required to force the non-wetting liquid into the a pore is given by:

$$P = - (4 \gamma \cos \theta)/ D \qquad (11)$$

Where
P = apply pressure
γ = surface tension of the non-wetting liquid
θ = contact angle between the liquid and the solid sample
D = pore diameter

Cos θ is negative for non-wetting liquid. In this technique, the pressure and volume of intruded non-wetting liquid are measured and recorded by the instrument. Thus pore diameter, pore volume, and pore volume distribution can be computed. If the absolute volume of a sample is known, the sample porosity can be calculated accordingly.

Density Measurement with Gas Pycnometer

The absolute volume and density can be measured with a gas pycnometer. Gas has very low surface tension and can easily fill up very small pores and voids. The volume and density measured should be close to real volume and density of the sample if fraction of closed pores is insignificant. Gas pycnometer measures the volume of solid objects of regular or irregular shapes whether powdered or in one piece. A gas pycnometer consists of a sample cell chamber and an expansion chamber with a control valve connecting the chambers. The working equation [4] is

$$V_{samp} = V_{cell} - V_{exp}/((P_{1g}/P_{2g}) - 1)) \qquad (12)$$

Where
V_{samp} = volume of the sample
V_{cell} = volume of cell chamber (known)
V_{exp} = volume of expansion chamber (known)
P_{1g} = gauge pressure of cell chamber when the valve is closed
P_{2g} = gauge pressure of cell chamber when the valve is open

Calibration is performed to determine V_{cell} and V_{exp} before sample volume is measured.

Mechanical Property Measurement Using Ultrasound Probe

Material property characterization using standard ultrasonic wave propagation techniques requires measurement of both the shear and longitudinal sound speeds through the material. To accomplish these measurements, material samples of known thickness, in conjunction with a means to generate and detect sonic waves of the two types, are required. By determination of the

times-of flight (TOF) along a path of known distance, the sound speeds may be estimated. Generally, separate measurements are made for each wave type.

Once measurements of the shear and longitudinal wave speeds of a particular material have been achieved, a series of calculations may be performed to estimate mechanical properties. Several equations, derived from linear elastic theory, are used. In these equations the only additional parameter required, aside from the two wave speeds, is the material density. Some of the properties that may be calculated include the shear modulus, Young's modulus, the bulk modulus, and Poisson's ratio. Note that Poisson's ratio depends only on the ratio of the two wave speeds and is independent of the density.

The equations used to calculate these values are as follows [5].

Young's Modulus:

$$E = r\, C_S^2\, (3C_l^2 - 4C_S^2)/(C_l^2 - C_S^2) \quad (13)$$

Bulk Modulus: $$K = r\, [C_l^2 - (4/3)C_S^2] \quad (14)$$

Shear Modulus: $$G = C_S^2\, r \quad (15)$$

Where
r = material density, kg/m^3
C_s = materials shear sound speed as measured, m/s
C_l = materials longitudinal sound speed as measured, m/s

The moduli are in GPa. The above equations yield results that are accurate where the assumptions of linear elastic behavior apply.

Burn Rate

Measurement of liner burn rate of explosives can be made in a strand burner. Liner burn rate is expressed by the following equation [6].

$$B = a\, P^n \quad (16)$$

Where
B = liner burn rate, mm/s
a = burn rate coefficient, (mm/s)/(MPa^n)
P = pressure at the surface of the burn front, MPa
n = burning rate index, dimensionless

EXPERIMENTAL METHOD

Un-confined Thermal Damage Experiments

A remotely controlled portable oven (Figure 2) was built that provides desired ramp rates and permits a good control of oven temperature within ± 3 C at 190 ^{o}C and within ± 4 C at 250 ^{o}C, respectively. It is a useful device for conducting unconfined thermal damage experiments. It consists of a sample chamber, coil heaters, several temperature elements (5 RTDs, 3 thermocouples), and a control system. The sample chamber was made of a 6" pipe with a copper bottom plate and a removable top blank flange. Heating coils are placed underneath the copper plate and on the top flange. Samples are placed in several aluminum pans (2" OD) sitting on the copper plate. The portable oven was installed in a 1 kg shot tank when the thermal experiment was conducted. This was a required safety precaution for any unwanted explosion.

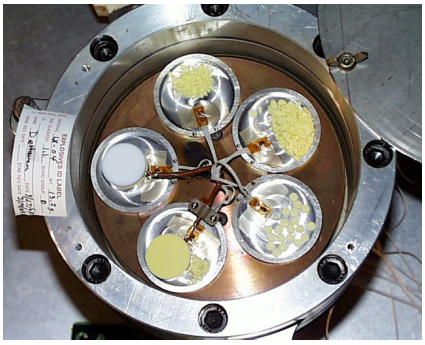

FIGURE 2. Portable oven for unconfined thermal damage experiments

Experimental Conditions For Heating LX-04, LX-10 And LX-17

Before conducting thermal damage experiments, a calculation was done to determine the critical temperature and times to explosion at different temperatures. The information allowed us to determine a safe operational envelop for thermal damage experimentation. Table 1 describes the process conditions for the three explosives. A minimum safety factor of 3 was used for heating time. Safety factor (SF) is the ratio of soak time to the calculated time to explosion; SF > 3 recommended.

TABLE 1. Process conditions for thermal damage experiments

Material	Soak temperature. °C	Soak time, hours	Safety factor
LX-04	140	22	∞
	190	2	> 3
LX-10	180	4	> 6
LX-17	190	4	∞
LX-17	250	2	> 12

Characterization of Pristine and Damaged Materials

Several material properties (density, sound speed, gas permeability, porosity, surface area, burn rate) of pristine and damaged samples were measured and characterized. Most of the samples were characterized at room temperature except for some gas permeability measurements and burn rate measurements which were performed in-situ, i.e. right after thermal damage experiments were done and samples were at high temperature. Some of damaged samples were also evaluated for their sensitivities to impact, friction and spark.

RESULTS AND DISCUSSIONS

Sample Discoloring, Density, and Dimensions

Sample exposure at high temperatures resulted in significant discoloring but negligible weight loss. Dimensions and weights of some cylindrical pressed parts were carefully measured before and after thermal experiments, as shown in Table 2 and Table 3 for LX-04 and LX-17, respectively. Weight losses after thermal treatment were insignificant (less than < 0.5%). Samples expanded significantly after thermal exposure at 190 °C. The bulk density of LX-04 decreased by 0.27% and 7.17% at 140 °C and 190 °C, respectively. For LX-17, bulk density decreased by 4.08% and 8.01% at 190 °C and 250 °C, respectively. The results suggest that the samples have become more porous after heating.

TABLE 2. LX-04 Sample volume and bulk density after thermal damage

Sample	Wt., g	Vol., cc	Bulk density, g/cc	%TMD
Pristine LX-04	3.5616	1.9181	1.857	98.3
140 °C, 22 hrs	3.5600	1.9214	1.852	98.04
% Change	-0.045	+0.72	-0.27	
Pristine LX-04	3.5605	1.9206	1.854	98.14
190 °C, 2 hrs	3.5550	2.0662	1.721	91.08
% Change	-0.154	+7.579	-7.17	

TABLE 3. LX-17 Sample volume and bulk density after thermal damage

Sample	Wt., g	Vol., cc	Bulk density, g/cc	%TMD*
Pristine LX-17	9.7379	5.1183	1.9024	97.86
190 °C, 4 hrs	9.7289	5.3316	1.8248	93.87
% Change	-0.090	+4.16	-4.08	
Pristine LX-17	9.7364	5.0967	1.9103	98.27
250 °C, 2 hrs	9.726	5.5272	1.7572	90.39
% Change	-0.240	+8.45	-8.01	

* TMD is theoretical maximum density

Estimate of Total Porosity and Fractions of Closed Pores and Open Pores

Micrometer can measure dimension and volume of certain samples; the resulting density is often called bulk density because closed pores, blind pores, and through pores are not included in the measurement. Blind pores and through pores are open pores since they are reachable by gas molecules. The gas pycnometer uses gas displacement principle with a gas pressure of 20 psig and the density obtained from the measurement is called true density. It is very closed to theoretical maximum density (TMD) of the sample if the fraction of closed pores in the sample is insignificant. Several small LX-10 pressed parts thermally damaged at 180 °C for 4 hours and sample volumes were measured with

micrometer and pycnometer. Total porosity, fraction of closed pores, fraction of open pores can then be estimated as follows.

$$\varepsilon = (TMD - \rho_b)/TMD \quad (17)$$

$$f_c = (TMD - \rho_t)/TMD \quad (18)$$

$$f_o = \varepsilon - f_c \quad (19)$$

Where ε = total porosity, dimensionless
f_c = fraction of closed pores; dimensionless
f_o = fraction of open pores; dimensionless
ρ_b = bulk density, g/cc
ρ_t = true density, g/cc

Table 4 shows the total porosity, fraction of closed pores, fraction of open pores of LX-10 samples after the thermal exposure for 4 hours at 180 °C. The samples became much more porous, evidenced by the increase of total porosity from 2.2% to 14.37%. Much of the porosity increase came from the open pores (20 times), although fraction of open pores also increased significantly. At this point, light scattering techniques (small angle neutron scattering or small angle X-ray scattering) or porosimetry has not been used to measure porosity and pore size distribution for this work. Nonetheless, the use of pycnometer and micrometer can be useful approximation of porosity measurement.

TABLE 4. Porosity, fraction of closed pores, fraction of open pores of LX-10 samples

Sample	ρ_b, g/cc	ρ_t, g/cc	ε, %	f_c, %	f_o,%
Pristine LX-04, 0.3679 g	1.8543 97.80% TMD	1.8624 98.23% TMD	2.20	1.77	0.43
Damaged, 0.3666 g	1.6235 85.63% TMD	1.8158 95.77% TMD	14.37	4.23	10.14
% Change	- 12.45%	- 2.50%	+12.17	2.46	9.71

Sound Speeds and Moduli

Thermal exposure may increase porosity that can result in lower sound speeds in energetic materials. This may mechanically weaken energetic materials. An ultrasound probe was used to monitor sound speeds in the LX-04 and LX-17 pristine and damaged samples. With sound speeds and density data, moduli of the material can be computed from equations 13, 14, and 15. The results are listed in Figures 3 & 4, respectively. The moduli of the damage samples dropped significantly after thermal damage. It indicates the materials are mechanically much weaker after thermal exposure.

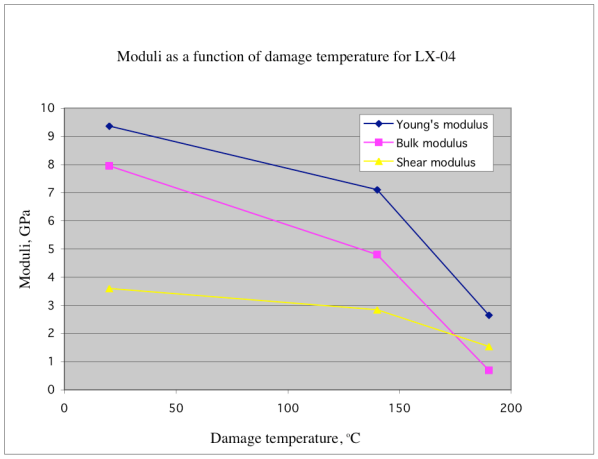

FIGURE 3. LX-04 moduli drop after thermal exposure at high temperatures

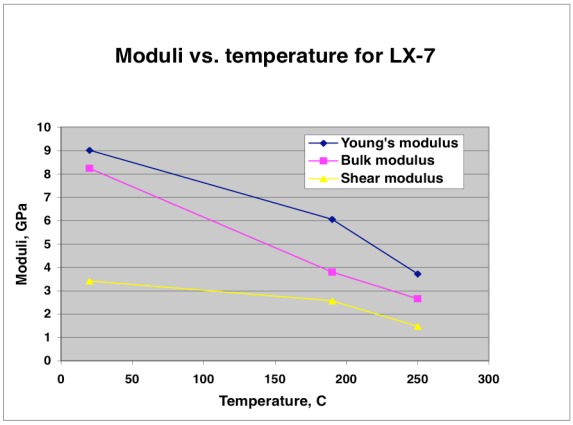

FIGURE 4. LX-17 moduli drop after thermal exposure at high temperatures

Gas Permeability in Explosives

Most of the exothermic energy release of explosive decomposition occurs in the gas phase and thus it is essential to know how the hot gaseous products move through the remaining network of HMX particles. The most important physical parameter, both experimentally and for input to reactive flow computer models [7], is the permeability of the solid explosive to gas flow under all possible conditions. Gas permeation in explosives is highly dependent of material density and porosity. We have recently made some gas permeability measurements in a newly procured permeation system (diffusion permeameter) as shown in Figure 5. It measures gas permeability in pressed parts from 10^{-20} m^2 to 10^{-12} m^2, with sample dimensions up to 2" in diameter and thickness up to 0.4". The design operational temperature of the system is 250 ^oC. Detailed description of the system has been published elsewhere [8].

We measured gas permeabilities at room temperature on some pristine and thermally damaged pressed parts of LX-04, LX-10, and LX-17. Results are shown in Table 5. Damaged pressed parts were results of thermal exposure at high temperatures in an un-confined environment. The samples were then glued to stainless steel holders at room temperature. All samples were 1" in diameter and up to 0.2" in thickness. The glue we used was checked carefully to make sure that it is leak-free at temperatures up to 200 ^oC. Table 5 shows that gas permeabilities in the high density samples (98% TMD) of pristine LX-04 and LX-17 were below the detection limit of the system (10^{-20} m^2). Both pristine LX-10 and PBX 9501 samples, both consisting of 95% HMX, show low but detectable gas permeabilities. Gas permeability is highly dependent of material density. Table 5 shows gas permeability of pristine LX-10 increases by 4 orders of magnitude as density decreases from 98% TMD to 89% TMD. Thermal damage at high temperature can induce voids, reduce density, and increase gas permeability by 2 orders of magnitude or greater, depending heating temperature, duration, and confinement. As high as 5 orders of magnitude increase in gas permeability was observed with PBX 9501 [9,10].

We also measured gas permeability in-situ for LX-04, LX-07, and LX-10 at high temperatures. Pristine parts were at room temperature potted to the holder, heated to pre-determined temperatures and soaked for several hours. The samples were radially-confined as they were heating up. Table 6 shows that gas permeability in hot samples is several orders of magnitude higher than that in pristine samples at room temperature. LANL also reported similar results for PBX 9501 [9,10].

Figure 6 shows the gas pressures in the downstream chamber for LX-04 and LX-07 permeability experiments. Gas permeation through the LX-07 sample was very significant after the sample was heated at 175 ^oC for 3 hours. No detectable gas permeation was observed in the pristine high-density (98% TMD) samples of LX-04 and LX-07 at room temperature. More measurements are underway for collecting gas permeability data at high temperatures for different materials.

FIGURE 5. Diffusion Permeameter

TABLE 5. Gas permeability measured at room temperature

Sample description	Density, g/cc	Gas Permeability m^2	Note
Pristine LX-04	98.3% TMD	$< 10^{-20}$	Below the detection limit
Damaged LX-04, unconfined heating at 140 ^oC for 22 hours	98.0% TMD	$< 10^{-20}$	Below the detection limit
Damaged LX-04, unconfined heating at 190 ^oC for 2 hours	91.8% TMD	1.8×10^{-18}	
Pristine LX-10	97.9% TMD	6.2×10^{-18}	
Pristine LX-10	94.8% TMD	6.6×10^{-16}	
Pristine LX-10	91.8% TMD	3.6×10^{-15}	
Pristine LX-10	89.3% TMD	1.1×10^{-14}	
Pristine LX-17	98.0%	$< 10^{-20}$	Below the detection limit
Pristine LX-17	91.9%	2.8×10^{-17}	
Damaged LX-17, unconfined heating at 250 ^oC for 2 hours	90.4%	5.4×10^{-18}	
Pristine PBX 9501	98.0% TMD	4.2×10^{-19}	LANL data [9,10]
Damaged PBX 9501, unconfined heating at 180 ^oC for > 2 hours	-	6.9×10^{-14}	LANL data [9,10]

Note: Damaged samples were potted after they were thermally damaged and cooled to room temperature

TABLE 6. Gas permeability measured at room temperature and high temperatures

Sample description[1]	Gas Permeability at room temperature m^2	Gas Permeability at 175 ^oC[2] m^2	Note
LX-04	$< 10^{-20}$	5.4×10^{-17}	Density 98.3% TMD at room temperature (pristine)
LX-07	$< 10^{-20}$	1.2×10^{-15}	Density 98.0% TMD at room temperature (pristine)
LX-10	6.2×10^{-18}	- (in progress)	Density 97.9% TMD at room temperature (pristine)
LX-17	$< 10^{-20}$	- (in progress)	Density 98.0% TMD at room temperature (pristine)
PBX-9501	4.2×10^{-19}	2.9×10^{-16} measured at 180 ^oC	LANL data [9,10]

Notes:
1. Pristine samples were potted with stainless steel holder at room temperature
2. Samples were soaked for 3 hours

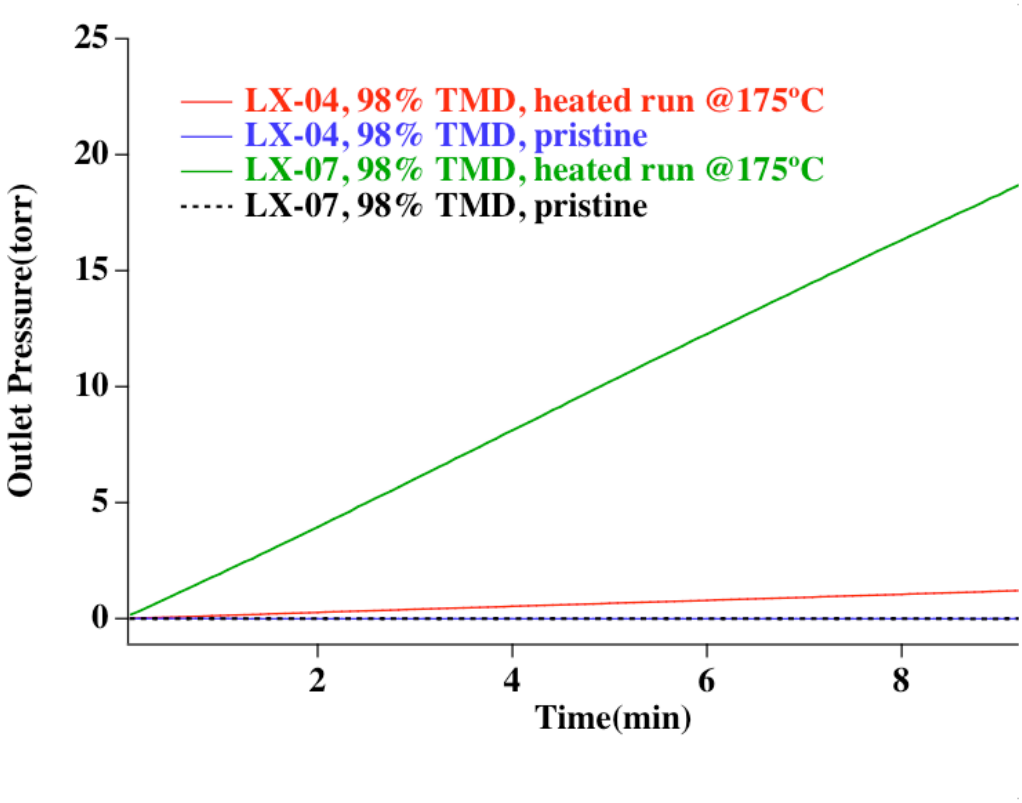

FIGURE 6. Downstream pressure vs. time for LX-04 and LX-10 permeability measurements

Surface Area

Gas adsorption technique (BET) was used to measure surface areas of pristine and damaged powders. The BET system we used at LLNL can measure samples of low surface area (< 1.0 m^2/g) with argon as adsorbate. Figure 7 shows a reduction in surface area of LX-17 powder after thermal exposures at high temperatures. The reason for the surface area reduction is not clear at this time. More study is needed. Surface area of pressed parts was not measured by the BET system.

Safety and Sensitivity of Damaged Materials

Damaged materials may be more sensitive to impact, friction or shock. Urtiew et. al [11] reported that LX-04 was more sensitive to shock at elevated temperatures as shown in Figure 8. Run distance to detonation was much shorter for heated samples as they were hit at high temperature by a high-speed impactor.

Small- scale safety tests (drop hammer, friction) were also used to determine sensitivity of damaged samples after they were cooled to room temperature. No significant sensitization was observed for the cool damaged samples, as shown in Table 7 and Table 8. Only slight increase in friction sensitivity for cool damaged LX-04 was observed. The reason is not clear at this time. More study is needed.

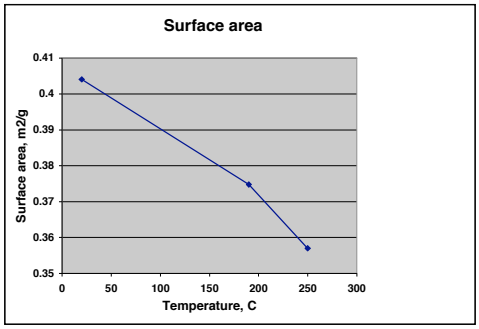

FIGURE 7. Surface area of LX-17 powder

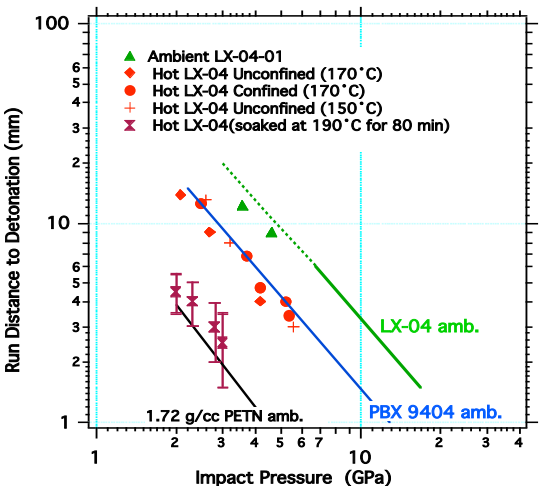

FIGURE 8. "Pop Plot" for heated LX-04 showing its sensitivity to impact as compared to other sensitive high explosives

TABLE 7. Small-scale safety test data on heated and then cooled LX-04 samples

Test	Ambient LX-04	140˚C for 22 hours	190˚C for 2 hours
Drop hammer, cm	84	74	119
Friction	0/10 @ 36 kg	1/10 @ 32 kg	1/10 @ 36 kg
DSC, ˚C	284.4	283.5	283.3

TABLE 8. Small-scale safety data on heated and then cooled LX-17 samples

Test	Ambient LX-17	190˚C for 4 hours	250˚C for 2 hours
Drop hammer, cm	> 177	>177	>177
Friction	0/10 @ 36 kg	0/10 @ 36 kg	0/10 @ 36 kg
DSC, ˚C	380.4	383.7	382.9

LX-10 Burn Rate Measurements

Burn rates were measured in the LLNL high-pressure strand burner (Figure 9). It was designed to handle burn rate measurements for pressures up to 1,000 MPa and temperatures up to 300 ^{o}C. Detailed description of the system can be found elsewhere [12]. We used the system for thermal damage in-situ followed by burn rate measurement. Small pressed pellets were assembled into a burn tower that was heated in the pressure chamber of the system for several hours. Temperature spread on the burn tower surface from top to the bottom was controlled at ± 1.5 C. We conducted several thermal damage experiments on LX-10 at 150 ^{o}C, 180 ^{o}C, 190 ^{o}C, and 195 ^{o}C, respectively. Burn rates were measured right after thermal damage experiments and results are shown in Figure 10.

Burn rates of damaged LX-10 at 180 ^{o}C (4 hours) were 2 to 3 orders of magnitude faster than those of pristine LX-10 due to the effect of higher degree of damage and phase transition from beta to delta. Burn rates of damaged LX-10 at 150 ^{o}C are only slightly faster than those of pristine LX-10. For the heated runs above 190 ^{o}C, self-ignition occurred. Deflagration was obvious with LX-10 at ambient burns at pressure above 150 MPa. This was consistent with previous studies [12]. For heated runs at 180 ^{o}C, deflagration occurred at lower pressure due to the thermal damage. Thermal damage can lead to higher porosity, higher surface area, and faster burn rates. The increase in surface area and vivacity can be estimated from burn rates and has been reported by Koerner et. al. [13].

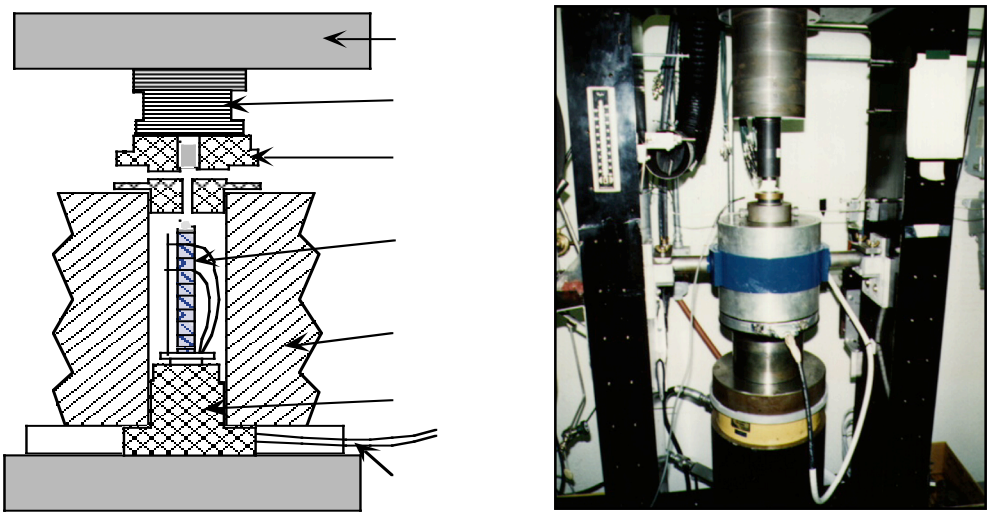

(a) (b)

FIGURE 9. LLNL High-pressure strand burner (a) schematic (b) picture of the system

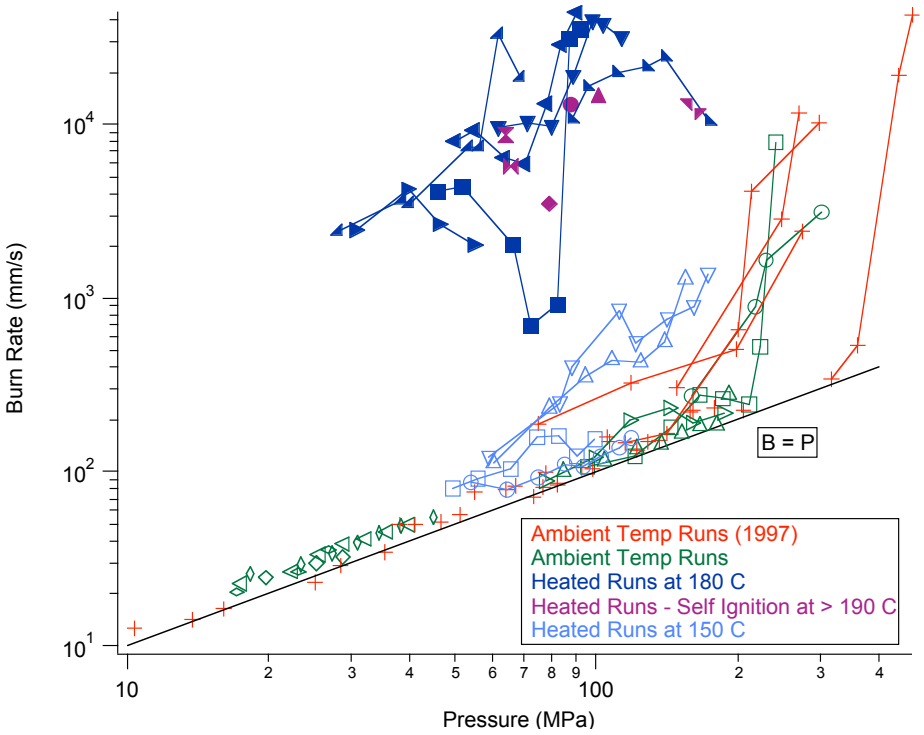

FIGURE 10. LX-10 burn rate

CONCLUSIONS

In order to evaluate the effect of thermal insults, we conducted thermal damage experiments on LX-04, LX-10, and LX-17 and characterized material properties. Thermal treatment leads to de-coloring but small weight losses. Volume expansion at high temperatures was significant and led to reduction in material density. Gas permeation measurement showed that gas permeability in damaged materials was several orders of magnitude higher than that in pristine materials. Damaged energetic materials may be more sensitive to shock at higher temperatures. Small-scale safety tests (DSC, impact, and friction) showed no significant sensitization when these heated samples were tested at room temperature. It also appeared that thermal damage had profound effect on sound speeds in the damaged pressed parts. It indicated the samples became weaker mechanically as sound speeds in materials dropped. We also measured burn rates of thermally damaged materials in a strand burner and found that burn rates were 2 to 3 orders of magnitude faster than those of pristine materials. In summary, we have found that thermal insults changed material properties significantly.

ACKNOWLEDGEMENTS

We would like to thank members of Thermal Response Group for helping with thermal experiments. The sound speed was measured by Bruce Cunningham. Funding from the HE Response Program in the Defense and Nuclear Technology is greatly appreciated. This work was performed under the auspices of the U.S. Department of Energy by the University of California Lawrence Livermore National Laboratory under contract No. W-7405-Eng-48.

This paper has been reviewed and released for unlimited distribution, UCRL-CONF-222392.

REFERENCES

1. Bird, R.B., Stewart, W.E., and E.N. Lightfoot, *Transport Phenomena*, publisher, and place of publication, pp. 150, 1960.
2. Daniels, F., and Albert, R.A., "Physical Chemistry", 3rd edition, 1966.
3. Lecture Notes and Short Course, Porous Materials, Inc., Ithaca, 2002.
4. 1330 Pycnometer Operator's Manual, Micromeritics Instrument Company, 2003.
5. Cunningham, B., Harwood, P., and Healy, T., "Material Property Measurements on PBX and Other Materials Using Ultrasonics" Lawrence Livermore National Laboratory, 2001.
6. Cooper, P.W., and Kurowski, S.R., *Introduction to Technology of Explosives*, Wiley-VCH , pp 42, 1996.
7. Private communication with Dr. Craig Tarver, Lawrence Livermore National Laboratory, 2003.
8. Hsu, P.C., DeHaven, M., McClelland, M., and Maienschein, J.L. "THERMAL DAMAGE ONLX-04 MOCK MATERIAL AND GAS PERMEABILITY ASSESSMENT" *Propellants, Explosives, Pyrotechnics* Vol. 31, No. 1, pp 56-60, 2006.
9. Asay, B.W., Parker, G., Dickson, P., Henson, B., and Smilowtz, L., "DYNAMIC MEASUREMENT OF THE PERMEABILITY OF AN EXPLOSIVE UNDERGOING THERMAL DAMAGE" *J. Energetic Materials*, Vol. *21*, pp 25, 2004.
10. Asay, B.W., Schaefer, T., Dickson, P., Henson, B., and Smilowtz, L.,, "*Measurement of Gas Permeability of Thermal Damaged PBX 9501"* Los Alamos National Laboratory Report LAUR-02-1755, Los Alamos, NM, USA., 2002.
11. Urtiew, P.A., Forbes, J.W., Tarver, C. M., Vandersall, K.S., Garcia, F., Greenwood, D.W., Hsu, P.C., and Maienschein, J.L. "SHOCK SENSITIVITY OF LX-04 CONTAINING DELTA PHASE HMX AT ELEVATED TEMPERATURES" Conference Proceeding, APS National Meeting, Portland, Oregon, July 2003.
12. Maienschein, J.L., Wardell, J.,DeHaven, M., and Black, K. "DEFLAGRATION OF HMX-BASED EXPLOSIVES AT HIGH TEMPERATURES AND PRESSURES" *Propellants, Explosives, Pyrotechnics* Vol. 29, No. 5, pp 287, 2004.
13. Koerner, J., Maienschein, J.L., DeHaven, M., and Kevin Black, to be presented in the 13th International Detonation Symposium, 2006.